Localization of matter waves in lattice systems with moving disorder

Chenyue Guo,[1] Wenhao Cui,[1] and Zi Cai[1,2,*]

[1]*Wilczek Quantum Center and Key Laboratory of Artificial Structures and Quantum Control, School of Physics and Astronomy, Shanghai Jiao Tong University, Shanghai 200240, China*

[2]*Shanghai Research Center for Quantum Sciences, Shanghai 201315, China*

(Received 24 January 2022; revised 11 February 2023; accepted 21 February 2023; published 28 March 2023)

We study the localization phenomena in a one-dimensional lattice system with a uniformly moving disordered potential. At a low-moving velocity, we find a sliding localized phase in which the initially localized matter wave adiabatically follows the moving potential without diffusion, thus resulting in an initial state memory in the many-body dynamics. Such an intriguing localized phase distinguishes itself from the standard Anderson localization in two aspects: it is not robust against interaction, but persists in the presence of slowly varying perturbations. Such a sliding localized phase can be understood as a consequence of interference between the wave-packet paths under moving quasiperiodic potentials with various periods that are incommensurate with the lattice constant. The experimental realization and detection are also discussed.

DOI: 10.1103/PhysRevA.107.033330

I. INTRODUCTION

The absence of the diffusion of waves in a disordered medium (dubbed Anderson localization) originates from the interference between various scattering paths, thus it is ubiquitous in wave physics [1]. Such a phenomenon is expected to be robust against weak interactions, and has reattracted enormous interest recently in the context of many-body localization (MBL) [2–5]. Even though disorders naturally exist in solid-state settings, they can also be artificially introduced into intrinsically clean systems (e.g., the ultracold atom or trapped ion) in a controllable matter [6,7]. Owing to its unique features such as the perfect isolation and high degree of parameter tunability [8], the cold-atom system represents a new perspective for studying localization [9–12]. For instance, it allows the exploration of localization physics in a far-from-equilibrium system within a strong driving regime inaccessible in conventional solid-state settings [13–16], and thus is beyond the scope of the linear response theory derived by Mott [17].

In cold-atom experiments, a quantum many-body system can be driven out of equilibrium by periodically or stochastically modulating the system parameters. Recently, an intriguing driving protocol other than a regular (periodic) or completely irregular (stochastic) driving protocols was proposed [18]. Therein, neither a spatial translational symmetry nor a temporal translational symmetry (TTS) are present for the driving potential, which, instead, exhibits nontrivial intertwined space-time symmetries that cannot be decomposed into a direct product of spatial and temporal symmetries. Owing to the absence of discrete TTS, such a driving protocol significantly differs from the periodic driving, thus the widely employed Floquet description no longer applies, nor does it resemble the stochastic or quasiperiodic ones [19–22] due to its strong correlation along a particular space-time direction.

Such an intriguing driving protocol avails new possibilities exploring nonequilibrium physics beyond the scope of periodically driven systems [23–25]. As an example, in this study, we explore the localization physics in a driven-disordered system with a sliding space-time translational symmetry (SSTS). The proposed system is a one-dimensional (1D) quantum model subjected to a time-dependent inhomogeneous potential as a superposition of a dynamic disordered potential moving at a constant velocity and a static periodic one (see Fig. 1). As will be demonstrated, such a moving disordered potential with tunable velocity can be readily achieved in the cold atomic systems, even though it is unrealistic in solid-state settings. Contrary to the periodically driven disordered systems which are generally delocalized by low-frequency perturbations [14,26–29], in the proposed model, a sliding localized phase (SLP) was observed at a sufficiently low velocity of the moving potential. Even though the center of mass (COM) of the matter wave adiabatically follows the moving potential, it does not cause diffusion. Such an SLP persists in the noninteracting many-body systems, which exhibit an initial state "memory" effect. However, dissimilar to the MBL systems, SLP will be delocalized even by weak interactions. The system is delocalized at a high moving velocity. Moreover, instead of diffusion, we find a ballistic transport in the single-particle dynamics and an algebraic decay of the initial state memory at the many-body level.

II. MODEL AND METHOD

First, we considered a time-dependent single-particle Hamiltonian, which is defined in the 1D continuum space as follows:

$$\hat{H}(x,t) = \frac{\hat{p}^2}{2m} + V_s(x) + \tilde{V}(x,t), \tag{1}$$

where $V_s(x) = V_s(x+a)$ is a static periodic potential that is produced by the optical lattice with lattice constant a. $\tilde{V}(x,t)$

*zcai@sjtu.edu.cn

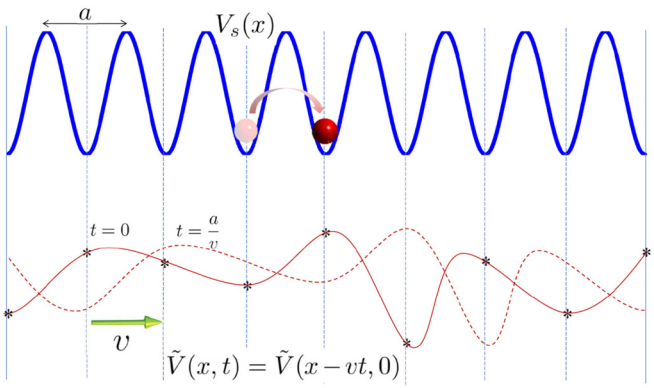

FIG. 1. Schematic of the static periodic and moving disordered potentials in our model.

represents the time-dependent disordered potential that breaks the spatial translational symmetry at any given time. To drive the system out of equilibrium, the disordered potential is suddenly pushed forward at a constant velocity **v** indicating $\tilde{V}(x,t)=\tilde{V}(x-vt,0)$. The explicit form of $\tilde{V}(x,t)$ would be formulated subsequently. $\hat{H}(x,t)$ preserves the SSTS even though it breaks the temporal and spacial translational symmetry separately

$$\hat{H}(x,t)=\hat{H}(x+a,t+a/v). \tag{2}$$

Provided the static periodic potential is sufficiently deep, we adopted the single-band approximation and derived the tight-binding Hamiltonian in the 1D lattice as

$$\hat{H}(t)=\sum_i[-J(C_i^\dagger C_{i+1}+\text{H.c.})+V_i(t)\hat{n}_i], \tag{3}$$

where C_i ($C_i^\dagger$) is the annihilation (creation) operator of the spinless fermion on site i and $\hat{n}_i=C_i^\dagger C_i$. J is the nearest-neighboring (NN) single-particle hopping amplitude and $V_i(t)=\tilde{V}(x=ai,t)$ is the moving disordered potential at time t. Assuming $V_i(t=0)$ was randomly sampled from a uniform random distribution with $V_i(t=0)\in[-\Delta,\Delta]$. To recover the continuum function $\tilde{V}(x,t=0)$ from a set of given points $\{V_i(t=0)\}$, we performed cubic spline interpolation to smoothly connect these points on the different sites, and derived the continuum function $\tilde{V}(x,t=0)$. The results did not significantly depend on specific interpolation methods (see Appendix A). Immediately after determining $\tilde{V}(x,t=0)$, $V_i(t)$ at any given time can be obtained using the identities $\tilde{V}(x,t)=\tilde{V}(x-vt,0)$ and $V_i(t)=\tilde{V}(x=ai,t)$. Despite the similarity in their SSTS, we should emphasize that the proposed potential is significantly different from that in the space-time crystal [18,30] since our potential has only one lattice vector as shown in Eq. (2), thus it is not a crystal in the 1 + 1-D space time.

III. SINGLE-PARTICLE DYNAMICS

We first consider the single-particle situation, where the initial state was chosen as the ground state of Hamiltonian (3) with $t=0$. Starting from such a spatially localized wave packet, we study the time evolution of the wave function $|\psi(t)\rangle$ by directly solving the time-dependent Schrödinger equation with different moving velocities. The density distributions $\rho_i(t)=\langle\psi(t)|\hat{n}_i|\psi(t)\rangle$ during the time evolution were plotted in Fig. 2(a), which revealed that the COM of the wave packet $X(t)=\sum_i i\rho_i(t)$ could not catch up with the moving potential at a relatively high velocity [$X(t)<X(0)+vt$ as shown in Fig. 2(b)]. Consequently, the wave packet experienced a sequence of rapidly varying disordered potentials, which consistently perturbed the wave packet stochastically as noise and finally delocalized it. This delocalization can be characterized by the width of the wave packet $w(t)=\sqrt{\sum_i\rho_i(t)[i-X(t)]^2}$. Figure 2(c) shows that $w(t)$ roughly grows linearly after a long time, indicating a ballistic transport [$w(t)\sim t$] rather than diffusion [$w(t)\sim t^{\frac{1}{2}}$] reported previously in noisy disordered systems [20,31]. This discrepancy exists because the SSTS [Eq. (2)] resulted in a strong space-time correlation for the disorder-induced "noise," thus stopping it from being "white" noise. Such a ballistic transport resembles the dynamics of the disorder-free case, indicating that a fast-moving disordered potential does not qualitatively change the long-time dynamics of lattice systems, it only renormalizes the hopping amplitude J.

The situation is qualitatively different at a low velocity. Figure 2(b) shows that the COM adiabatically followed the moving potential [$X(t)=X(0)+vt$], while its width $w(t)$ was bounded even after sufficiently a long time [see Fig. 2(c)], indicating the absence of diffusion. The uniform motion of COM and the absence of the diffusion of the wave packet were the main features of SLP at the single-particle level. The existence of the SLP indicates the validity of the adiabatic theorem in our model (see Appendix D). The localization or delocaliztion of a wave packet does not only depend on the moving velocity, but also on the initial state energy. For instance, if we begin from another eigenstate of $\hat{H}(t=0)$ close to the band edge, the physics is similar as analyzed above, while for an initial state in the band center, even an infinitesimal velocity would be sufficient to delocalize the wave packet. Consequently, for a given velocity, a critical initial energy exists to separate the sliding localized and delocalized states. The existence of such a critical initial energy is crucial for our subsequential discussion regarding the many-body cases with and without interactions.

It is helpful to compare our results with the wave-packet dynamics under a suddenly moving single trap. For instance, the dynamics of a bound state in the presence of a uniformly moving attractive δ potential (with a velocity v) can be solved exactly [32], which showed that the wave packet will be split into three parts with different velocities: one adiabatically follows the moving trap at a velocity v, while the other two escape from the trap (with a velocity 0 and $2v$, respectively) and there is no dynamics phase transition. In our model, the two wave packets escaping from the original trap will be localized by the disordered potential in the SLP, thus the wave packet will adiabatically follow the moving potential.

IV. MANY-PARTICLE DYNAMICS WITHOUT INTERACTION

One of the valuable features of localization is the memory effect of the initial-state information, which will be partially preserved during time evolution. For instance, if we

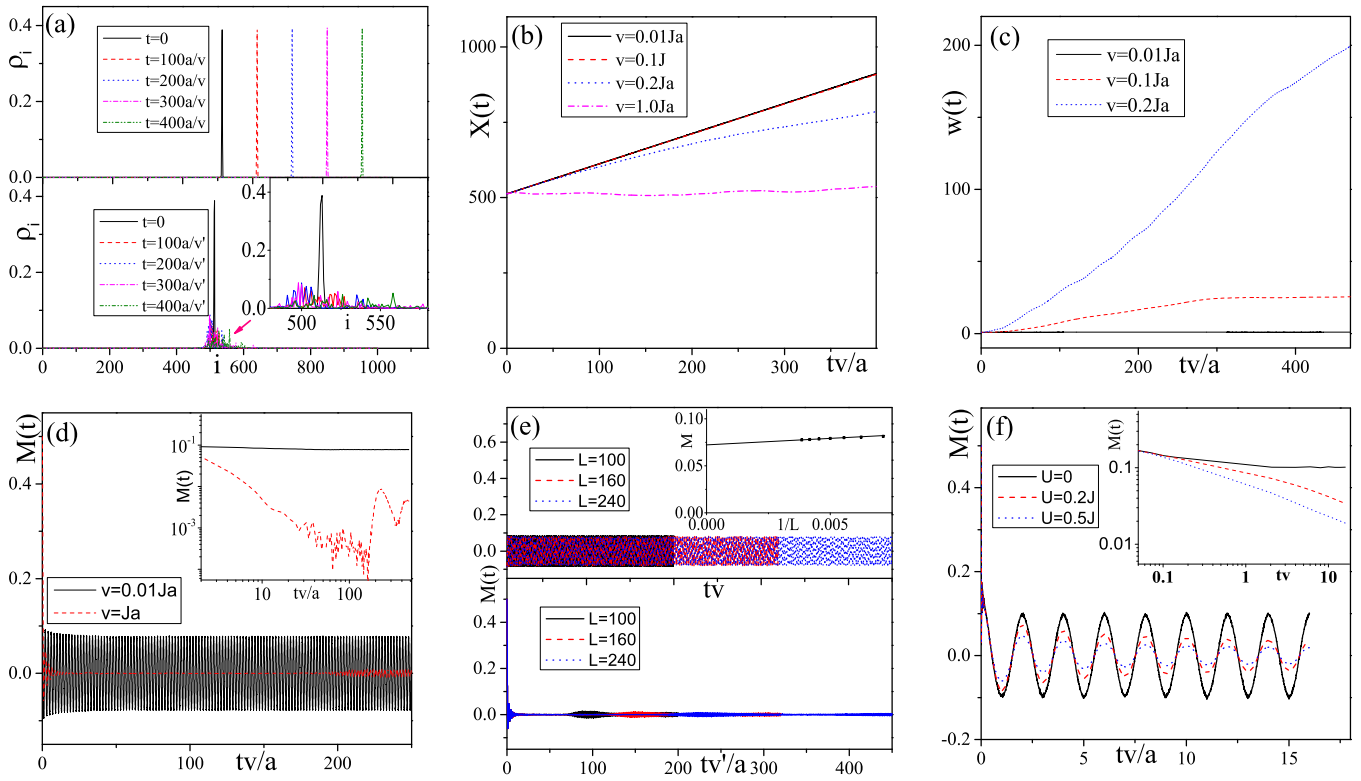

FIG. 2. (a) Density distributions of the wave packet at different time slices during the single-particle dynamics in the SLP ($v = 0.01Ja$) and delocalized phase ($v = Ja$). The inset magnifies the lower panel. Evolution of the (b) COM and (c) width of the wave packet under different moving velocities. Here and hereafter, tv rather than t would be employed to characterize the evolution time, thus allowing the comparison of the dynamics with different v on the same footing. (d) Comparison between $M(t)$ in SLP ($v = 0.01Ja$) and delocalized phase ($v = Ja$) during the noninteracting many-body dynamics beginning from the same ($|1010\cdots\rangle$) initial state. The inset is the envelope of the oscillations in (d) in a log-log plot. (e) Dynamics of M(t) in the noninteracting systems with different system sizes L for the SLP ($v = 0.01Ja$ for the upper panel) and delocalized phase ($v' = Ja$ for the lower panel). The inset is a finite-size scaling of the amplitudes of the persistent periodic oscillations (M) in the SLP ($v = 0.01Ja$). (f) Dynamics of $M(t)$ in the small systems with different NN interaction strengths U. The inset is the envelope of the oscillations in (f) in a log-log plot. The system sizes are chosen as $L = 1000$ for (a)–(c), $L = 240$ for (d) and $L = 16$ for (f). The discrete time step $\Delta t = 0.001J^{-1}$ for all the cases except $v = 0.01Ja$ where $\Delta t = 0.01J^{-1}$ and $\Delta = 4J$ for (a)–(f). A random disorder realization was selected for (a)–(c) and the ensemble averages over 300 disorder realizations were performed for (d)–(f). [a] indicates in the unit of lattice constant a.

begin from a half-filled charge-density-wave (CDW) state $|1010\cdots\rangle$, the density imbalance between two sublattices of the 1D lattice $M(t) = \frac{1}{L}\sum_i (-1)^i \rho_i(t)$ in the initial state would be memorized [$M(t \to \infty) \neq 0$] in localized phases [12], however, in the delocalized phase, it would be washed out after extended period [$M(t \to \infty) \to 0$]. Thus, to characterize the feature of SLP from the perspective of many-body physics, we selected the $|1010\cdots\rangle$ initial state and studied the time evolution under the noninteracting Hamiltonian (3) with different v by solving the equation of motion of the equal-time single-particle Green's function $G_{ij}(t) = \langle\psi(t)|C_i^\dagger C_j|\psi(t)\rangle$, from which all the physical quantities at any given time, including $M(t)$, were derived.

Without interaction, the dynamics of the many-body (fermionic) systems can be understood as the collective behavior of different single-particle states, each of which evolves independently. At a low velocity, the system adiabatically followed the moving potential, so is the CDW state. A CDW state moving at a constant velocity can be characterized by the persistent periodic oscillation of $M(t)$ [Fig. 2(d)]. Notably, the oscillation amplitude is smaller than that in the initial state [$M(0) = 0.5$], which can be explained by the aforementioned delocalized single-particle states that barely contribute to the sliding CDW order. $M(t)$ in systems with different system sizes were plotted in Fig. 2(e). Therein, a finite-size scaling (see the inset and Appendix A) shows that such periodic oscillations in SLP persisted in the thermodynamic limit. Although such a sliding CDW state resembles the "moving solid" proposed in the steady states of CDW systems driven by applied electric fields [33–35], there is a significant difference: the CDW order in the "moving solid" is induced by interactions, while that in our study originated from the initial state memory. At a high velocity, the long-time dynamics of $M(t)$ noticeably exhibited an algebraic decay $\sim t^{-\alpha}$ (accomplished by an oscillation) with a nonuniversal exponent α depending on v.

V. MANY-PARTICLE DYNAMICS WITH INTERACTION

To examine the effect of interaction on the SLP in our model, the NN interactions between fermions were introduced

as follows:

$$\hat{H}_I(t) = \sum_i [-J(C_i^\dagger C_{i+1} + \text{H.c.}) + V_i(t)\hat{n}_i + U\hat{n}_i\hat{n}_{i+1}], \quad (4)$$

where U is the strength of the NN interaction. Employing the exact diagonalization method, the time evolution of $M(t)$ was studied beginning from the $|1010\cdots\rangle$ state under the Hamiltonian (4) for a relatively small system ($L = 16$) and compared with the noninteracting case. Figure 2(f) shows that even a weak interaction in the SLP ($v = 0.01J$) can delocalize the system and lead to an algebraic decay of $M(t)$. This is strikingly different from the static disorder-induced localization, which is generally robust against weak interaction. Such an interaction-induced delocalization can also be explained by the aforementioned critical initial energy, above which the single-particle states are delocalized. Generally, the interaction would induce scatterings between the different single-particle states, thus mix the localized and delocalized states. Therefore, those delocalized states above the critical initial energy act as a bath that is coupled to the localized states and delocalize the whole system.

VI. DISCUSSION

Under Fourier transformation $\tilde{V}(x,t) = \frac{1}{\sqrt{L}}\sum_k V_k e^{ik(x-vt)}$, the moving disorder potential turns to a superposition of a set of moving periodic potentials with different wavelengths, which are typically incommensurate with the lattice constant a. Therefore, to understand the SLP, one should first focus on the dynamics of a particle in the presence of a moving quasiperiod potential (qPP) with a period incommensurate with a. Regarding the static case ($v = 0$), it is known that a sinusoidal qPP with $\Delta > 2J$ would also result in a localization that is similar to the Anderson localization in the disordered system [36]. Thus, their dynamical behaviors in the presence of the moving potential could be expected to be similar. However, Fig. 3(a) shows this is not the case. In the presence of a slowly moving qPP $V_{k_0}(x,t) = \Delta\cos 2\pi k_0(x - vt)$ with $v = 0.01J$, starting from the initial state as the ground state of $V_i = V_{k_0}(ia, 0)$, the variance of the wave packet $w(t)$ is plotted in Fig. 3(a) (the solid black curve), which grows linearly with time, indicating a ballistic transport behavior similar with that of disorder-free case.

The delocalization of a particle under a slowly moving qPP can be understood via the Landau-Zener tunneling (LZT) [37]. Considering a qPP with a period a_0 incommensurate but slightly larger than a, and further assuming that initially the minima of the qPP and lattice potential coincide at site i, we choose the initial state as the ground state at $t = 0$, which is spatially localized around site i. Since a_0 is slightly larger than a, the potential energies on site i and $i \pm 1$ at $t = 0$ are close to each other but separated from those on other sites. We focus on site i and $i - 1$ whose potential energies vary with the movement of qPP. As shown in Fig. 3(b), at time $t^* = \frac{a_0 - a}{v}$, the energy minimum is shifted from site i to $i - 1$ [$V_{i-1}(t^*) = V_i(0)$], indicating an energy level crossing. Considering the particle tunneling between site i and $i - 1$, this physics resembles the Landau-Zener tunneling: for a slow moving velocity $v \ll J$, the wave packet will follow the energy minimum thus tunnel from site i to site $i - 1$ at $t = t^*$. With further movement of qPP, the wave packet will keep tunneling, thus give rise to a ballistic transport with a renormalized tunneling rate depending on t^* see Appendix D.

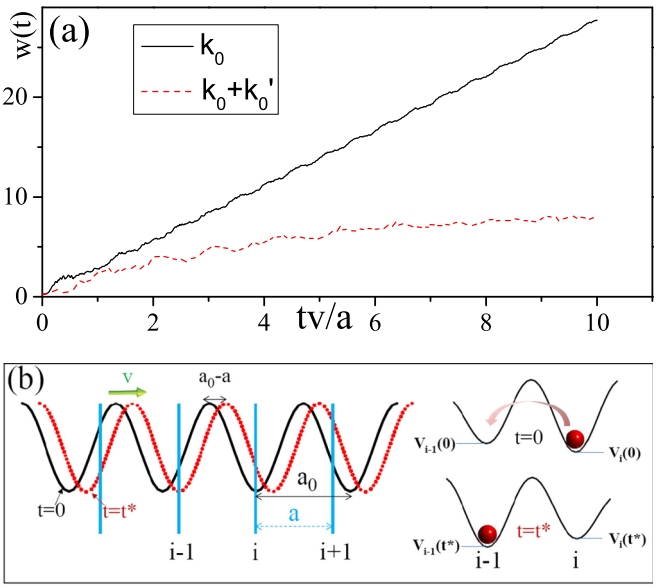

FIG. 3. (a) Comparison between the dynamics of the width of wave packet in the presence of a single-moving quasiperiodic potential $V_{k_0}(x,t) = \Delta\cos 2\pi k_0(x - vt)$ with and a superposition of two quasiperiodic potentials $V'_{k_0}(x,t) = \frac{\Delta}{2}[\cos 2\pi k_0(x - vt) + \cos 2\pi k'_0(x - vt)]$. The parameters are chosen as $\Delta = 4J, L = 1000$, $v = 0.01Ja$, $k_0 = \frac{\sqrt{5}-1}{2}$, and $k'_0 = \frac{\sqrt{6}-1}{2}$. (b) Sketch of the nearest-neighboring tunneling of the wave packet induced by a moving qPP during the period $[0, t^*]$ with $t^* = \frac{a_0 - a}{v}$.

This picture is helpful for us to understand the SLP in the moving disordered potential, which can be considered as a superposition of moving qPPs with different a_0. For a single qPP, a wave packet tunneling from site i to $i - 1$ carries a phase depending on the tunneling time t^*, which in turn is determined by a_0 of the qPP. Therefore, in the presence of many qPPs with random a_0, the wave packets carrying different phases will interfere with each other at site $i - 1$, thus suppressing the effective tunneling and lead to localization. This point can be numerically verified by comparing the dynamics of $w(t)$ with a single qPP and more than one qPP. As shown in Fig. 3(a), in the presence of two qPPs with different periods, $w(t)$ significantly deviates from the linear growth, indicates that the effective tunneling is strongly suppressed.

The qualitatively different dynamics behavior between the cases with slow and fast moving velocities indicates there exists a localized-to-delocalized phase transition. However, based on the LZT picture, one may argue that at a small velocity (e.g., $v = 0.01Ja$ as chosen here), the heating rate is exponentially small, thus is beyond the numerical precision in our simulation. As a consequence, the observed localized phase is not actually localized, but a delocalized phase with extremely slow spreading. To check this point, we choose another moving velocity $v = 0.05Ja$ and calculate the energy

absorption in this case. As shown in Appendix E, we find there is no qualitative difference between the cases with $v = 0.01Ja$ and $v = 0.05Ja$: at sufficiently long time, the energy of the system still saturates and we have not observed any signature of slow heating in this case. This result, although not a rigorous proof, suggests that the proposed sliding localized phase is indeed a stable phase that exists in a finite regime of the phase diagram. However, due to the limit of the finite size and simulation time in our numerical simulation, it is difficult to preclude the possibility of a delocalized phase with extremely slow spreading.

VII. EXPERIMENTAL REALIZATION AND DETECTION

The proposed model can be experimentally simulated by loading atoms into a quasi-1D optical lattice, in which the disordered and quasiperiodic potentials can be introduced in controllable ways: the first was realized by by implementing a speckle potential generated by a laser beam passing through a diffusion plate [6,10], while the second can be introduced by imposing an additional optical lattice whose period is approximately incommensurate with that of the original one [11]. In both cases, the moving potentials could be realized by shifting either the diffusion plate or the phase of the additional lasers at a constant velocity. For an optical lattice with $a = 512\,\text{nm}$ and $J \simeq 400\,\text{Hz}$, one can estimate that the realistic moving velocity corresponds to the typical parameter regime discussed above is in the order of a magnitude of $10\,\mu\text{m/s}$. Regarding the detections, the density imbalance $M(t)$ can be be directly or indirectly measured via the superlattice band-mapping technique [38] or heterodyne detection method, respectively [39,40].

VIII. CONCLUSION AND OUTLOOK

In summary, the dynamics of quantum systems with moving disordered potentials were studied and a sliding localized phase, which availed a new perspective for studying of driven-disordered systems, was clarified. This result can apply to matter waves in a wide range of wave phenomena in disordered media [41–43]. Future developments will include generalization or extension of our findings to higher-dimensional systems in which the motion of disordered potentials along a certain dimension might produce intriguing anisotropic localized phases in which the matter wave is delocalized along the driving direction, but still localized along other directions that are perpendicular to it. A more general question is whether there exists an effective time-independent description analog to the Floquet Hamiltonian for this type of driven systems with intertwined space-time symmetry. If there exists any, what are the "local" integrals of motions that account for the initial state memory in the sliding localized phase? Finally, even though we focused on localization physics, the proposed driving protocol can be studied in a broader context, especially in the interacting quantum systems where the interplay between the spontaneous symmetry breaking and the moving disorder might give rise to nontrivial phenomena, e.g., a generalization of the Imry-Ma arguments [44] for the robustness of symmetry breaking to such a moving disorder.

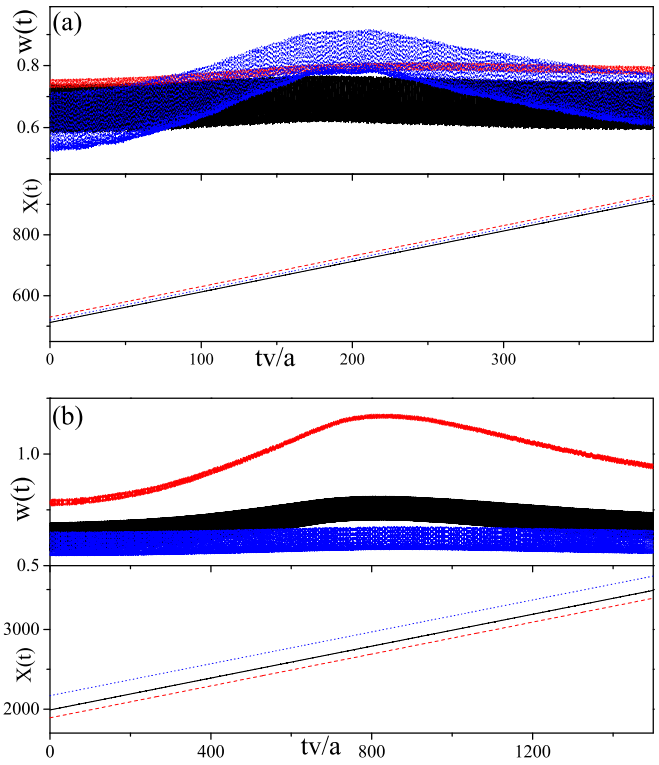

FIG. 4. The time evolution of width (upper panel) and COM (lower panel) of the wave packets under three different disorder realizations with system size (a) $L = 1000$ and (b) $L = 4000$, $v = 0.01Ja$, and $\Delta = 4J$.

ACKNOWLEDGMENTS

This work is supported by the National Key Research and Development Program of China (Grant No. 2020YFA0309000), NSFC of China (Grant No. 12174251), Natural Science Foundation of Shanghai (Grant No. 22ZR142830), Shanghai Municipal Science and Technology Major Project (Grant No.2019SHZDZX01).

APPENDIX A: DETAILS OF THE NUMERICAL SIMULATIONS

In this section, we check the dependence of the sliding localized phase on different disorder realizations, system sizes, and spline interpolations.

1. Disorder realizations

In the main text, the single-particle dynamics is calculated under a given set of randomly chosen disorder realization $\{V_i(t = 0)\}$, it is thus important to check that our results do not crucially depend on the choices of the disorder realizations. To this end, we calculate the dynamics of the center of mass (COM) and width of the wave packets for different disorder realizations $\{V_i(t = 0)\}$ starting from the initial state as the ground state of the corresponding Hamiltonian. Without losing generality, we choose those disorder realizations whose ground state locates close to the center of the 1D lattice to avoid the boundary effect during the evolution as possible as we can. As shown in Fig. 4(a), the

long-time dynamics of the wave packets with different disorder realizations are qualitatively identical: at a low velocity ($v = 0.01Ja$), the COMs of the wave packets under different disordered potential adiabatically follow the moving potential $X(t) = X(0) + vt$, while in all these cases, their widths keep oscillating within a finite regime, which indicates an absence of diffusion. Therefore, the existence of the sliding localized phases does not depend on the choices of the disorder realization.

2. System size dependence and localization length

The single-particle simulation in the main text is performed on a 1D lattice with finite system site ($L = 1000$), which also limits the maximum simulation time ($t_{\max} \sim La/v$), after which the wave packet will be bounced by the boundary of the 1D lattice under the open boundary condition. For a 1D system with periodic boundary condition, in principle, the COM of a wave packet located on a ring is ill defined. To avoid the boundary or finite-size effect, we choose those initial states localized close to the middle of the 1D lattice [$X(t = 0) \simeq L/2$] and the typical simulation time $T < t_{\max}/2$.

It is known that sometimes the localization phenomena may be sensitive to the system size, especially for the weak disordered cases where the localization length is long enough to be compatible to the system size. To make sure that the system size ($L = 1000$) and simulation time chosen in the main text are long enough to capture the physics of the infinite long-time dynamics of a system in the thermodynamic limit, here we study a larger system ($L = 4000$), which also allows us to simulate the dynamics with a longer time. The dynamics COM and the width of the wave packets in a system with $L = 4000$, $v = 0.01Ja$, but different disorder realizations are shown in Fig. 4(b), from which we can see that there is no qualitatively difference between the results of $L = 4000$ and $L = 1000$ shown in Fig. 4(a).

In the single-particle dynamics, it is difficult to derive the localization length due to the intrinsic nonequilibrium nature of our model, which is different from the conventional Anderson localization or periodically driven systems where the localization length can be derived from the eigenstates of the single-particle (Floquet) Hamiltonian. In our model, there is no effective Hamiltonian description, thus the eigenstate analysis is invalid. However, as shown in the main text, the many-body dynamics of the sliding localized phase starting from the $|1010\cdots\rangle$ state will approach an asymptotic periodically oscillating dynamics, which allows us to study the equal-time single-particle correlation function $G(r,t) = \langle\psi(t)|\frac{1}{L}\sum_i C_i^\dagger C_{i+r}|\psi(t)\rangle$ in this asymptotic regime. We calculate $G(r,t)$ at two different time slices [t_1 and t_2 as shown in Fig. 5(a)], which, respectively, correspond to a wave peak and a wave node in the asymptotic oscillation regime. As shown in Fig. 5(b), both $G(r,t_1)$ and $G(r,t_2)$ rapidly (exponentially) decay in distance. By making an analog to the Anderson localization, such an exponential decay of the single-particle Green's function enables us to estimate the localization length (a few lattice constants), which is significantly smaller than the typical system sizes in our simulation (hundreds of lattice constants).

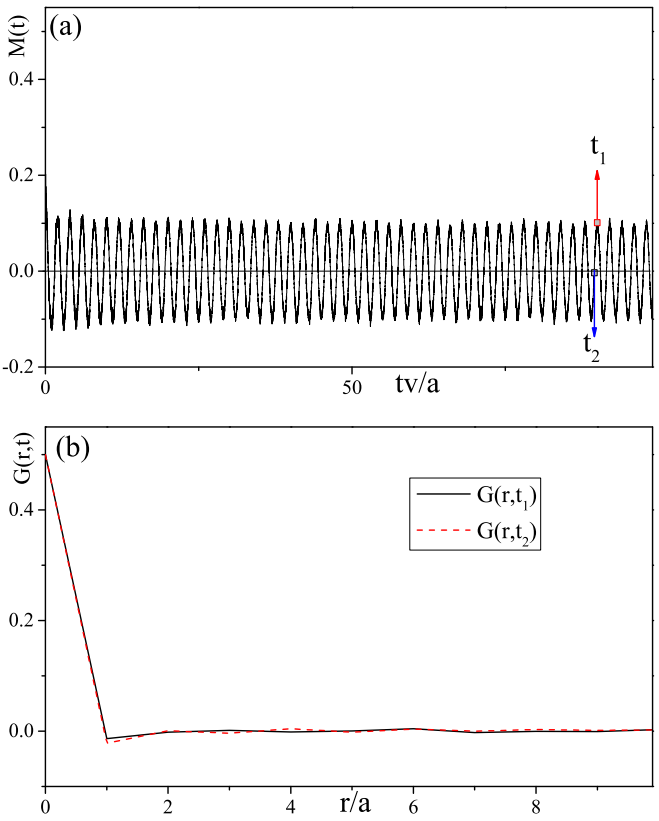

FIG. 5. (a) The dynamics of $M(t)$ for a noninteracting many-body system starting from the $|1010\cdots\rangle$ with parameters $L = 240$, $\Delta = 4J$, $v = 0.01Ja$. (b) The equal-time single-particle Green's function at two different time slices (t_1 and t_2), which, respectively, correspond to a wave peak and node of $M(t)$ as shown in (a). Ensemble average over 300 disorder realizations are performed in (a) and (b).

3. Finite-size scaling of the many-body dynamics

At half-filling case, the SLP is characterized by a persistent oscillation of the CDW order parameter $M(t) = \frac{1}{L}\sum_i(-1)^i\langle\Psi(t)|\hat{n}_i|\Psi(t)\rangle$ if we start from the initial state $|1010\cdots10\rangle$. As for the stability of the SLP, it is important to distinguish the persistent oscillation from an extremely slow decay and one needs to show that the oscillation amplitude does not decay to zero in the thermodynamic limit. To this end, we extended the simulation time of the many-body dynamics and provided some details of the finite-size scaling in this section. We plotted the envelop of the oscillations of $M(t)$ for different system sizes up to a sufficiently long time in In Fig. 6(a), from which we can find that $M_{en}(t)$ barely decays in time. We define the saturated amplitude M as the average of the $M_{en}(t)$ over the period $240a/v < t < 480a/v$ and study its dependence with system size. Figure 6(b) shows that M decays linearly with $1/L$, and in the thermodynamic limit, M extrapolates to a finite value, which indicates that the persistent oscillation does survive in the thermodynamics limit in the SLP.

4. Interpolation dependence

To recover the continuum potential function $\tilde{V}(x, t = 0)$ from a set of discrete points $\{V_i(t = 0)\}$ in our simulation we

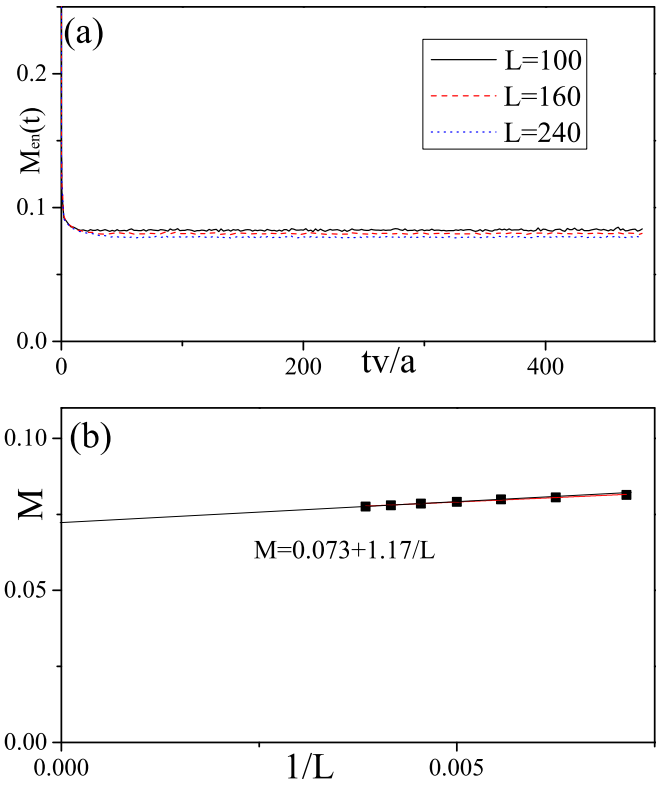

FIG. 6. (a) The envelop of $M(t)$ for different system sizes in the many-body dynamics of SLP. (b) Finite-size scaling of the saturated amplitude of the oscillation M. $\Delta = 4J$ and $v = 0.01Ja$ for (a) and (b). 300 disordered realizations are performed for each system size.

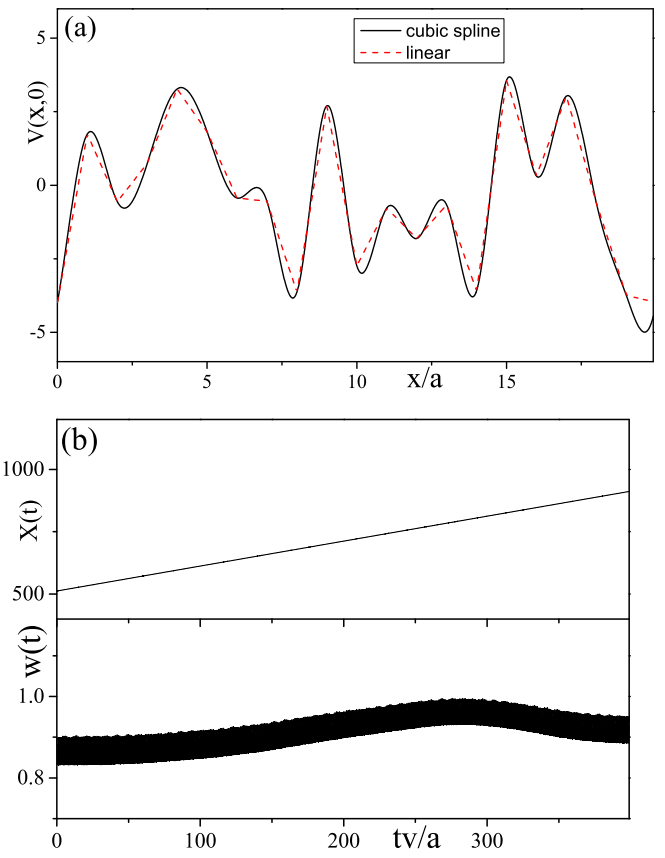

FIG. 7. (a) A comparison between the cubic spline interpolation and the linear interpolation from a same set of random $\{V_i(t=0)\}$. (b) The dynamics of COM (upper panel) and width (lower panel) of the wave packet under the moving potential $\tilde{V}(x,t)$ derived from the linear interpolation with parameters $L = 1000$, $\Delta = 4J$, $v = 0.01Ja$.

used the cubic spline interpolation to assure the smoothness of the function $\tilde{V}(x, t = 0)$. Here, we will show that our results does not crucially depend on such a specific choice of interpolation. To this end, we choose a different interpolation method [linear interpolation as shown in Fig. 7(a)] to derive $\tilde{V}(x, t = 0)$ from the same set of $\{V_i(t = 0)\}$ and calculate the dynamics of the wave packet under such a nonsmooth potential. As shown in Fig. 7(b) in spite of the roughness of the potential derived by linear interpolation, at a low moving velocity, the dynamics of the wave packet is qualitatively the same as that in the cubic spline interpolation, thus the existence of the sliding localized phase does not depend on the interpolation method. However, we should emphasize that the interpolated potential should be spatially continuous, otherwise it is impossible to define a adiabatic process. For instance, for a step-like potential $\tilde{V}(x) = V_i$, if $(i - \frac{1}{2})a < x < (i + \frac{1}{2})a$, there is no sliding localized phase no matter how slow the potential moves. Such a step-like moving potential is equal to the periodically kicked driving as we will analyze in the subsequential section.

APPENDIX B: OTHER DRIVING PROTOCOLS

1. Disordered potential with a periodically kicked driving

To the check the dependence of the SLP on the driving protocol of the disordered potential. We first consider a driving protocol with periodic kicks: instead of moving uniformly, within each driving circle, the disordered potential keeps static for a period of $\frac{a}{v}$ and then is suddenly pushed forward by a lattice constant. Mathematically, this disordered potential can be expressed as

$$V_1(x, t) = V[x - \theta(t), 0], \tag{B1}$$

with $\theta(t) = na$ for $(n - 1)a/v < t < na/v$. Notice that, on average, the disordered potential moving forward at a velocity v, however, the wave-packet dynamics under such a step-like driving protocol is qualitatively different from that under a uniformly moving disordered potential. As show in Fig. 8(a), at a low averaged velocity ($v = 0.01Ja$), the COM of the wave packet cannot follow the potential (it moves towards the opposite direction) and its width keep grows in time, indicating the absence of localization. The reason behind this is that there is no adiabatic limit for such a periodically kicked driving driving protocol no matter how small v is due to the sudden movement of the potential, thus it is impossible for the wave packet adiabatically following the moving potential.

2. Disordered potential with a periodically modulated amplitude

The second case considered involved a model of disordered potential with periodically modulated amplitude in which $\tilde{V}(x, t)$ takes the form of

$$V_2(x, t) = \cos vt \times \tilde{V}(x, 0), \tag{B2}$$

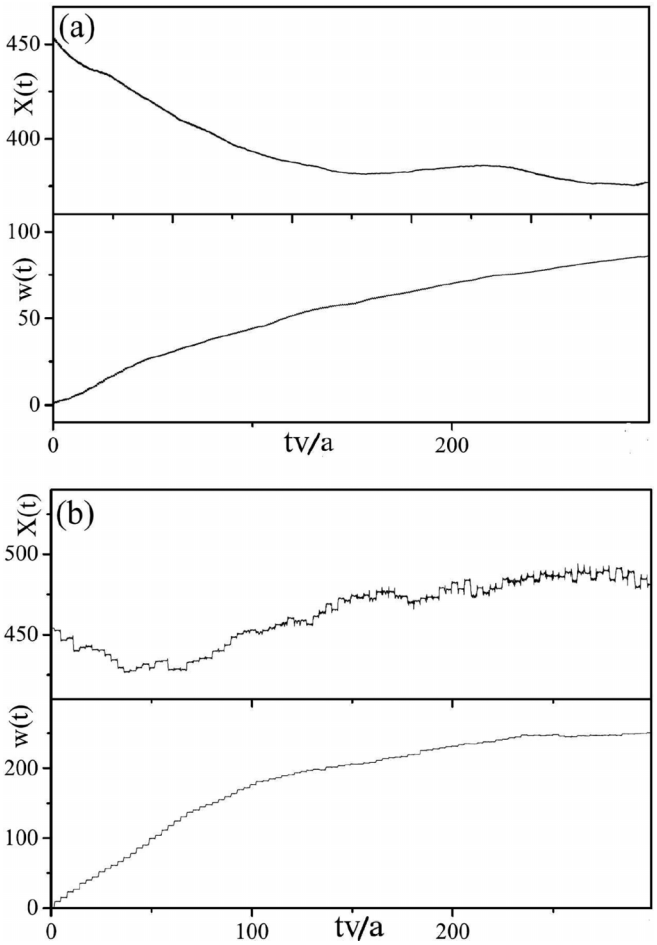

FIG. 8. (a) The dynamics of the COM $[X(t)$ in the upper panel] and width $[w(t)$ in the lower panel] of the wave packet in the presence of disordered potentials with (a) a periodical kicked driving and (b) a periodically modulating amplitude with the parameters $L = 1000$, $\Delta = 4J$, $v = 0.01Ja$. Neither of them exhibit the sliding localized phase at low v.

with $\tilde{V}(x, 0)$ being defined the same as in the main text. However, different from the moving disordered potential in the main text, $V_2(x, t)$ preserves the discrete temporal translational symmetry $V_2(x, t) = V_2(x, t + 2\pi/v)$. Figure 8(b) shows that, in the presence of such a periodically driven disordered potential, there is no localizations: the width of the wave packet keeps growing even in the presence of a low frequency $v = 0.01aJ$.

APPENDIX C: INITIAL STATE DEPENDENCE: EXISTENCE OF A CRITICAL INITIAL ENERGY

In this section, we will study the initial state dependence of the single-particle dynamics and show that the initial-state energy plays an important role in determining the long-time dynamics of the wave packet. We choose different initial states as the single-particle eigenstates of the Hamiltonian at $t = 0$, all of which are spatially localized in our 1D system. We use the energy E_n to characterize different initial states, where E_n is the eigenenergy of the nth eigenstate. As shown in Fig. 9(a), the long-time dynamics of the wave packet crucially depends

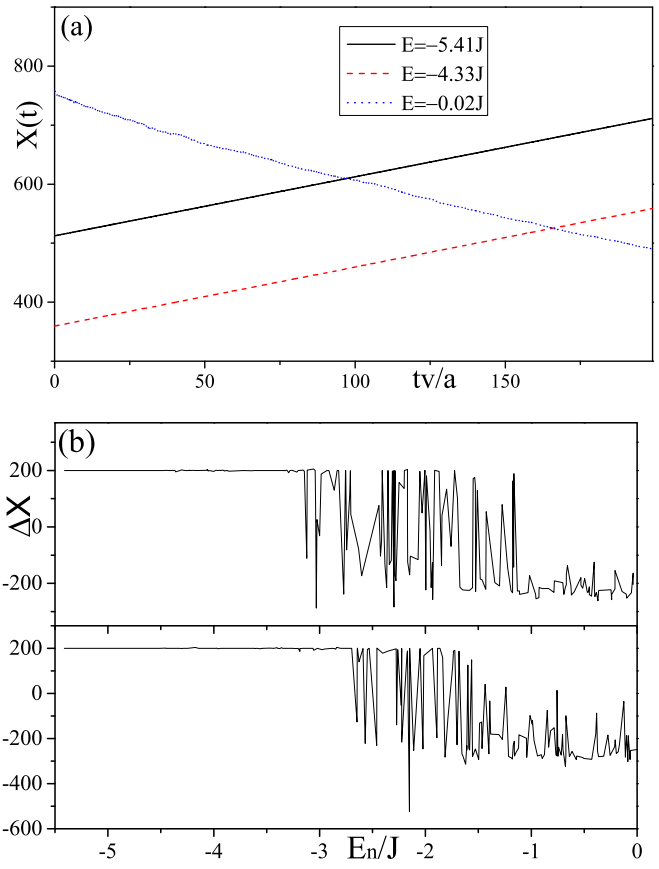

FIG. 9. (a) The dynamics of the COM of the wave packet starting from initial states with different eigen-energies for the initial state. (b) $\Delta X = X(T) - X(0)$ as a function of the initial state eigenenergy E_n with parameters $Tv = 200a$, $v = 0.01Ja$, and $L = 2000$ and two different disorder realizations (upper and lower panels).

on E_i: at a fixed (low) velocity ($v = 0.01aJ$), for those initial states close to the band edges (e.g., $E = -4.33J$), the long-time dynamics $[X(t) = X_0 + vt]$ are qualitatively identical to those starting from the ground state ($E = -5.41J$) and we still find a sliding localized phase, but with a lower critical velocity, while for those initial states close the band center (e.g., $E = -0.02J$), the COM of the wave packet does not follow the potential [it move towards the opposite direction of the potential as shown in Fig. 9(a)], and even an infinitesimal driving velocity can delocalize the system and induce a ballistic transport behavior.

For a given velocity, there exists a critical initial energy E_c to distinguish those sliding localized states from delocalized states. Numerically, the critical energy E_c is determined by the onset of the deviation of the adiabatic COM dynamics $[X(t) = X_0 + vt]$, which is always accompanied by the divergence of the width of the wave packet. For a fixed $v = 0.01Ja$, we plot $\Delta X = X(T) - X_0$ with $vT = 200a$ as a function of the eigenenergy E_n in Fig. 9(b), from which we can find $\Delta X = 200a$ for $E_n < E_c$, while for $E_n < E_c$, $\Delta X < 200a$. Figure 9(b) also suggests that the critical initial energy seems depends on the disorder realizations, but we are not sure whether such a dependence is a finite-size effect or not.

APPENDIX D: WAVE-PACKET DYNAMICS IN THE PRESENCE OF MOVING QUASIPERIODIC POTENTIAL

1. Ballistic transport and effective tunneling amplitude

In the main text, we show the wave-packet dynamics under a moving quasiperiodic potential is qualitatively different from that under a moving disordered potential, at a low velocity the moving disordered potential will be localized, while the moving quasiperiodic potential is characterized by a ballistic transport, where the width of the wave packet grows linearly with time. The slope of this linear growth can be considered as the velocity of the ballistic transport, which is proportional to the effective single-particle tunneling amplitude between adjacent sites (J'). As shown in Fig. 10(a), the slopes depend on the moving velocity of the potential from which we can derive a moving velocity dependence of the effective tunneling amplitude. Figure 10(b) suggests that J' depends on v in an oscillatory way whose envelop roughly grows linearly with increasing v. In the main text, we consider the situation where the period of the quasiperiodic potential (a_0) is slightly larger than the lattice constant (a). At a small moving velocity, the typical tunneling time between the adjacent sites is $t^* \sim \frac{a_0-a}{v}$, whereas the effective tunneling amplitude $J' \sim \frac{1}{t^*}$, thus is proportional to v. For a general a_0, the moving quasiperiodic potential may induce longer-range tunneling since the first excited state in this case may not locate at the adjacent sites of the ground-state wave packet.

2. Breakdown of adiabaticity in the presence of moving quasiperiodic potential

In the main text, we mentioned that the qualitatively different behaviors between the systems with moving disordered and quasiperiodic potential is related with the breakdown of the adiabaticity in the latter, here a detailed analysis of this point is provided. In general, for an isolated system with some external parameter being slowly driven from some initial value to the final one with a ramp speed v, assuming there is no energy level crossing on the way, the adiabatic theorem states that the excess entropy or energy density (δe) pumped into the system in this process as a function of v will approach to zero as $\delta e \sim v^2$ in the limit $v \to 0$. This is due to the fact that δe is an analytic function of v, but insensitive to its sign [$\delta e(v) = \delta e(-v)$].

Specific to our system, the time varying parameter is the phase shift $\phi(t)$ of the moving potential, which grows linearly as $\phi(t) \sim vt$, where the moving velocity v is the ramp speed. For simplicity, we consider the single-particle case. Initially, $\phi(t=0) = 0$ and we choose the initial state as the ground state of $\hat{H}(t=0)$. The final phase shift is chosen to satisfy the potential is pushed forward by one lattice constant $\phi(t=t_f) = a$, thus $t_f = a/v$. Due to the sliding space-time translational symmetry, the Hamiltonian at the final stage $\hat{H}(t=t_f)$ is equivalent to initial one $\hat{H}(t=0)$ by shifting one lattice constant ($i \to i+1$). Under the periodical boundary condition, this equivalence indicates that the energy spectrums of $\hat{H}(t=t_f)$ and $\hat{H}(t=0)$ are the identical with each other. As a consequence, the excess energy pumped into the system in this process (the disordered or quasiperiodic potential is pushed forward by one lattice constant) is defined as

$$\delta e = \langle \psi(t_f)|\hat{H}(t=t_f)|\psi(t_f)\rangle - E_0, \tag{D1}$$

where E_0 is the ground-state energy for both $\hat{H}(t=t_f)$ and $\hat{H}(t=0)$, which is also the system energy at $t=0$. $|\psi(t_f)\rangle$ is the wave function at the final time t_f.

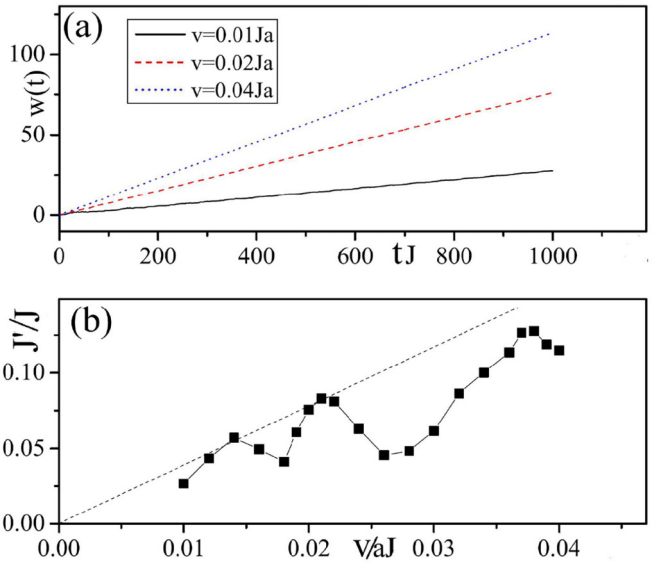

FIG. 10. (a) The dynamics of width of the wave packet in the presence of a slowly moving quasiperiodic potential $V_{k_0}(x,t) = \Delta \cos 2\pi k_0(x - vt)$ with different moving velocities. (b) The dependence of the renormalized nearest-neighboring tunneling amplitude [the slope of $w(t)$] as a function of moving velocity of the quasiperiodic potential. The parameters are chosen as $k_0 = \frac{\sqrt{5}-1}{2}$, $\Delta = 4J$, and $L = 1000$.

The excess energy δe as a function of v for both cases with disordered and quasiperiodic potential are plotted in Fig. 11(a), which indicates a qualitative difference between them: as for a moving disordered potential, the excess energy grows with the moving velocity as $\delta e \sim v^2$, which suggests that the adiabatical theorem still holds in this case. On the contrary, for the moving quasiperiodic potential $\delta e \to$ const. in the limit of $v \to 0$, indicating a breakdown of the adiabatical theorem, which can explain that even an infinitesimal velocity can delocalize the system. We expect that such a breakdown of the adiabatical theorem is due to the presence of a large amount of level crossings [∞L as shown in the inset of Fig. 11(b)] during this process, which pumps the particle to excited states via a sequence of Landau-Zener tunnelings. For a finite-size system, the level crossing as shown in Fig. 11(b) are actually separated by a small gap ΔE. However, it is worth mentioning that such a small gap decays exponentially with the system size [as shown in Fig. 11(c)] and will close in the thermodynamic limit.

APPENDIX E: ENERGY ABSORPTION

To distinguish the localization from a slowly spreading delocalization, we extend our simulation time up to $\mathcal{O}(10^2)$ times longer than that in the main text, and systematically study the dependence of the long-time behavior on the

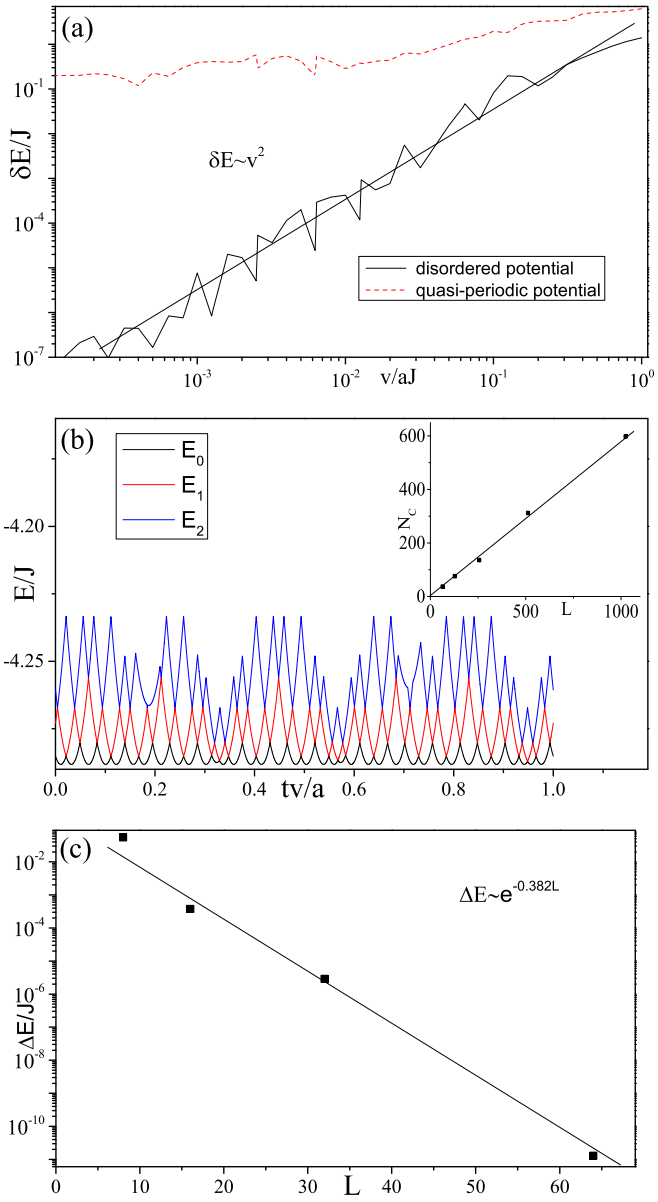

FIG. 11. (a) The excess energy pumped into the system after the potential is pushed forward by one lattice constant δE as a function of the moving velocity v in the presence of disordered or quasiperiodic potentials. (b) The instantaneous eigenenergies during this period $0 < tv < a$. The parameters are chosen as $L = 64$ and $\Delta = 4J$ for (a) and (b). The inset of (b) indicates the number of the energy crossing between the instantaneous ground state and first excited state as a function of the system size L. (c) The gap as a function of system size in the presence of moving quasiperiodic potentials.

simulation time, system size, and most importantly, the moving velocity.

1. Absorbed energy as a signature of localization or delocalization

In a previous study, we used the width of the wave packet to characterize the localization or delocalization. However, in the long-time dynamics, we are confronted with a dilemma: to study the dynamics of the wave packet, one needs to choose a 1D system with an open boundary condition (OBC) since the center of mass of the wave packet is ill defined in a 1D chain with periodic boundary condition (PBC) (e.g., an extensive wave packet with an uniform distribution within a ring). However, for the OBC, the simulation time is bounded since the wave packet should not be rebounded by the boundary during the evolution, otherwise the estimation of the width of the wave packet is not accurate. This dilemma indicates that the longest simulation time $\tau_{\max}$ in our previous simulation should be limited as $\tau_{\max} < \frac{La}{v}$.

To bypass this dilemma and study the longer-time dynamics, here we use the PBC but choose a quantity other than the width of the wave packet to characterize the localization or delocalization. The quantity we calculate is the absorbed energy $\Delta E(t) = E(t) - E_g$, where E_g is the initial energy [the ground-state energy of $H(t = 0)$] and $E(t)$ is the energy of the wave packet at time t. We only focus on the stroboscopic dynamics at $t_n = nt_0$, where n is an integer and $t_0 = a/v$ is a timescale during which the disordered potential is pushed forward by one lattice constant. Under PBC, the energy spectrum of $H(t_n)$ is exactly the same as that of $H(0)$ due to the translational symmetry, thus $\Delta E(t_n)$ represents the energy absorbed from the driving during the evolution. These quantities can be used to characterize localization or delocaliztion in this driving system: since we start from the site with lowest potential energy, if the wave packet is delocalized it will spread and its energy will keep growing until it reaches the upper bound of the single-particle energy $\sim\mathcal{O}(J)$. Otherwise, the wave packet will be localized around its original site and its energy will quickly saturate up to a value much smaller than $\mathcal{O}(J)$. It is known that the energy absorption rate is also considered as a signature of the dynamical localization in periodic driven systems [45–48].

2. Numerical results

In the following, we extend the simulation time up to a timescale of $10^4 a/v$ and systematically study the dependence of $\Delta E(t)$ on system size and moving velocity.

We first fix $v = 0.01aJ$ and study the long-time dynamics of $\Delta E(t)$ for different system sizes. Figure 12(a) shows that $\Delta E(t)$ will quickly saturate to a finite value $\sim\mathcal{O}(10^{-4}J)$, then oscillates around it. Physically, it means that the wave packet is breathing instead of spreading, which was also confirmed by our previous results of the dynamics of the width of the wave packet (Fig. 4). Within the timescale of our simulation ($10^6 J^{-1}$), there is no signature that $\Delta E(t)$ increases with time. Based on the numerical results, one can estimate that the heating rate, if it exists, should be much smaller than $10^{-10}J^2$. By comparing the results of various system sizes one can see that the saturate value of $\Delta E(t)$ does not significantly depend on the system sizes (it indeed depends on the disorder realization).

One may argue that the chosen velocity ($v = 0.01Ja$) is too small compared to the typical energy scale Δ_d between the ground and first excited state of the instantaneous Hamiltonian. ($\Delta_d \sim 0.1J$ for our model with the chosen parameters), thus the heating rate is exponentially small and indeed much smaller than $10^{-10}J^2$. To clarify this point, it is important to study another velocity that is compatible with Δ_d. To this

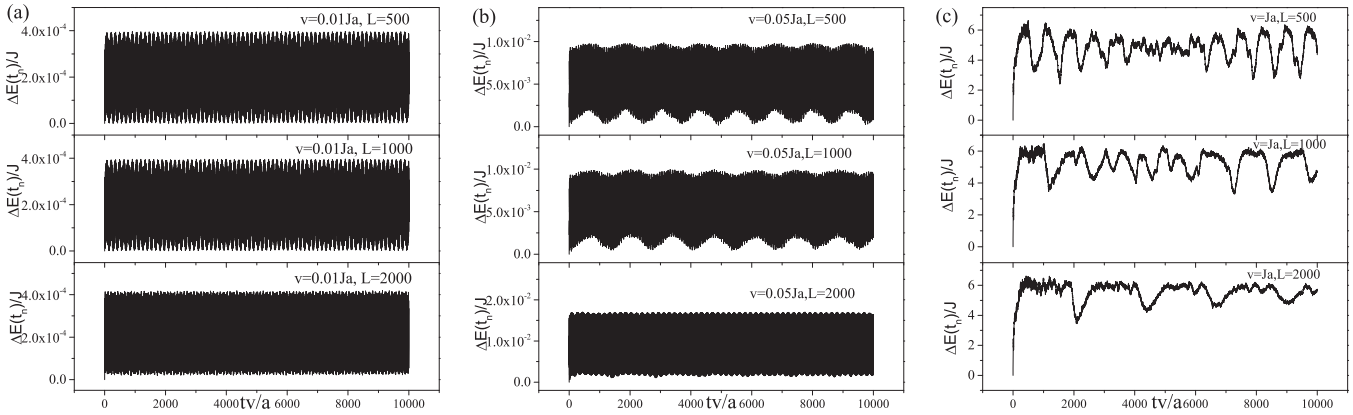

FIG. 12. The evolution of the absorbed energy $\Delta E(t_n)$ with different system sizes L and moving velocity v in the presence of moving disordered potential with $\Delta = 4J$.

end, we study the dynamics with $v = 0.05Ja$. As shown in Fig. 12(b), the saturated value of $\Delta E(t_n) \sim 10^{-2}J$ is larger than that in the case with $v = 0.01Ja$, but still much smaller than $\mathcal{O}(J)$, which indicates that even though the spatial distribution of the late-time wave packet with $v = 0.05Ja$ is boarder than that with $v = 0.01Ja$, it is still spatially localized. More importantly, from Fig. 12(b), one can see that, similar to the $v = 0.01Ja$ case, there is no heating signature up to the time scale of $10^4 a/v$. If the localization observed in the $v = 0.01Ja$ is an artifact of $v \ll \Delta_d$, one should expect a significant heating rate in the $v = 0.05Ja$ case where v is compatible to Δ_d, but this is not the case according to our numerical results.

As a contrast, we consider the dynamics of $\Delta E(t_n)$ at a fast moving velocity ($v = Ja$), where genuine delocalization occurs. As shown in Fig. 12(c), $\Delta E(t_n)$ also saturates after a sufficiently long time. However, the energy saturation in this case has a completely different origin from those in $v = 0.01Ja$ and $v = 0.05Ja$. As analyzed above, the second result is due to localization, while the first is due to the fact that there is an upper bound for the single-particle energy in such a 1D lattice system. The initial energy is $E(0) = -5.2J$, while Fig. 12(c) indicates that, after long-time $\Delta E(t_n)$ oscillates around $5J$, thus the final energy of the particle $[E(0) + \Delta E(t_n)]$ is $\mathcal{O}(0.1J)$. This value can be easily understood by the fact that, in the delocalized phase, the wave packet keeps absorbing energy from the driving until it is spread over all the lattice sites with random potential energies within $[-4J, 4J]$ (being most extensive) after sufficiently long time.

In summary, the qualitatively same long-time dynamics between the $v = 0.01Ja$ and $v = 0.05Ja$ cases indicates that the sliding localization state proposed in this study is indeed a robust "phase" that persists in a finite regime of the phase diagram.

[1] P. W. Anderson, Phys. Rev. **109**, 1492 (1958).
[2] D. M. Basko, I. L. Aleiner, and B. L. Altshuler, Ann. Phys. (NY) **321**, 1126 (2006).
[3] V. Oganesyan and D. A. Huse, Phys. Rev. B **75**, 155111 (2007).
[4] M. Žnidarič, T. Prosen, and P. Prelovšek, Phys. Rev. B **77**, 064426 (2008).
[5] A. Pal and D. A. Huse, Phys. Rev. B **82**, 174411 (2010).
[6] D. Clément, A. F. Varón, J. A. Retter, L. Sanchez-Palencia, A. Aspect, and P. Bouyer, New J. Phys. **8**, 165 (2006).
[7] A. Bermudez, M. A. Martin-Delgado, and D. Porras, New J. Phys. **12**, 123016 (2010).
[8] I. Bloch, J. Dalibard, and W. Zwerger, Rev. Mod. Phys. **80**, 885 (2008).
[9] L. Fallani, J. E. Lye, V. Guarrera, C. Fort, and M. Inguscio, Phys. Rev. Lett. **98**, 130404 (2007).
[10] J. Billy, V. Josse, Z. Zuo, A. Bernard, B. Hambrecht, P. Lugan, D. Clement, L. Sanchez-Palencia, P. Bouyer, and A. Aspect, Nature (London) **453**, 891 (2008).
[11] G. Roati, C. D. Errico, L. Fallani, M. Fattori, C. Fort, M. Zaccanti, G. Modugno, M. Modugno, and M. Inguscio, Nature (London) **453**, 895 (2008).
[12] M. Schreiber, S. S. Hodgman, P. Bordia, H. P. Luschen, M. H. Fischer, R. Vosk, E. Altman, U. Schneider, and I. Bloch, Science **349**, 842 (2015).
[13] P. Bordia, H. Luschen, U. Schneider, M. Knap, and I. Bloch, Nat. Phys. **13**, 460 (2017).
[14] O. S. Vershinina, E. A. Kozinov, T. V. Laptyeva, S. V. Denisov, and M. V. Ivanchenko, Europhys. Lett. **118**, 47004 (2017).
[15] D. T. Liu, J. T. Chalker, V. Khemani, and S. L. Sondhi, Phys. Rev. B **98**, 214202 (2018).
[16] M. M. Wauters, A. Russomanno, R. Citro, G. E. Santoro, and L. Privitera, Phys. Rev. Lett. **123**, 266601 (2019).
[17] N. Mott, Philos. Mag. **17**, 1259 (1968).
[18] S. Xu and C. Wu, Phys. Rev. Lett. **120**, 096401 (2018).
[19] P. T. Dumitrescu, R. Vasseur, and A. C. Potter, Phys. Rev. Lett. **120**, 070602 (2018).
[20] J. Ren, Q. Li, W. Li, Z. Cai, and X. Wang, Phys. Rev. Lett. **124**, 130602 (2020).
[21] D. M. Long, P. J. D. Crowley, and A. Chandran, Phys. Rev. B **105**, 144204 (2022).
[22] H. Zhao, F. Mintert, J. Knolle, and R. Moessner, Phys. Rev. B **105**, L220202 (2022).
[23] A. Eckardt, Rev. Mod. Phys. **89**, 011004 (2017).

[24] F. Harper, R. Roy, M. S. Rudner, and S. Sondhi, Annu. Rev. Condens. Matter Phys. **11**, 345 (2020).
[25] T. Oka and S. Kitamura, Annu. Rev. Condens. Matter Phys. **10**, 387 (2019).
[26] D. F. Martinez and R. A. Molina, Phys. Rev. B **73**, 073104 (2006).
[27] P. Ponte, Z. Papić, F. Huveneers, and D. A. Abanin, Phys. Rev. Lett. **114**, 140401 (2015).
[28] A. Lazarides, A. Das, and R. Moessner, Phys. Rev. Lett. **115**, 030402 (2015).
[29] D. A. Abanin, W. D. Roeck, and F. Huveneers, Ann. Phys. (NY) **372**, 1 (2016).
[30] Q. Gao and Q. Niu, Phys. Rev. Lett. **127**, 036401 (2021).
[31] S. Gopalakrishnan, K. R. Islam, and M. Knap, Phys. Rev. Lett. **119**, 046601 (2017).
[32] E. Granot and A. Marchewka, Europhys. Lett. **86**, 20007 (2009).
[33] A. E. Koshelev and V. M. Vinokur, Phys. Rev. Lett. **73**, 3580 (1994).
[34] A. C. Marley, M. J. Higgins, and S. Bhattacharya, Phys. Rev. Lett. **74**, 3029 (1995).
[35] L. Balents and M. P. A. Fisher, Phys. Rev. Lett. **75**, 4270 (1995).
[36] S. Aubry and G. Andre, Ann. Isr. Phys. **3**, 18 (1980).
[37] M. Wilkinson, J. Phys. A: Math. Gen. **21**, 4021 (1988).
[38] S. Trotzky, Y.-A. Chen, A. Flesch, I. P. McCulloch, U. Schollwöck, J. Eisert, and I. Bloch, Nat. Phys. **8**, 325 (2012).
[39] R. Landig, L. Hruby, N. Dogra, M. Landini, R. Mottl, T. Donner, and T. Esslinger, Nature (London) **532**, 476 (2016).
[40] L. Hruby, N. Dogra, M. Landini, T. Donner, and T. Esslinger, Proc. Natl. Acad. Sci. USA **115**, 3279 (2018).
[41] D. Wiersma, P. Bartolini, A. Lagendijk, and R. Righini, Nature (London) **390**, 671 (1997).
[42] R. L. Weaver, Wave Motion **12**, 129 (1990).
[43] R. Dalichaouch, J. Armstrong, S. Schultz, P. Platzman, and S. McCall, Nature (London) **354**, 53 (1991).
[44] Y. Imry and S.-K. Ma, Phys. Rev. Lett. **35**, 1399 (1975).
[45] M. Wilkinson and E. J. Austin, Phys. Rev. A **46**, 64 (1992).
[46] D. M. Basko, M. A. Skvortsov, and V. E. Kravtsov, Phys. Rev. Lett. **90**, 096801 (2003).
[47] S. Fishman, D. R. Grempel, and R. E. Prange, Phys. Rev. Lett. **49**, 509 (1982).
[48] D. R. Grempel, R. E. Prange, and S. Fishman, Phys. Rev. A **29**, 1639 (1984).